Data-Driven Optimization of Gyroid Energy Absorption

Eyan Documet, Jason Wang, and Solyana Beyene
University of California, Berkeley, Department of Mechanical Engineering, Berkeley, CA 94720, USA

Submitted: 12/15/2025.

Abstract
Gyroid structures are widely used in applications like additive manufacturing due to their nearly isotropic behavior and natural 3D tessellation, making them ideal for energy-absorbing applications (i.e. "crumple zones"). The isovalue T and the unit cell density d are two gyroid geometric parameters that influence the mechanical behavior of gyroids. We hypothesize that alterations to these two parameters will yield an optimum point where there is a highest amount of energy absorption per sample volume that is not trivially proportional to the amount of material used to fabricate the sample. This work examines the empirical relationship between these two parameters and the mechanical energy absorption of gyroid specimens fabricated across a range of parameter values. A full-factorial experimental design is employed in which the isovalue and the unit cell density are systematically varied as $T = \{0.25, 0.50, 0.75\}$ and $d = \{1, 2, 3\}$ respectively. These specimens are 3D printed with three replicates per configuration and placed into a custom quasi-static crush test method on an Instron machine. The data collected are thoroughly analyzed with multiple steps, including plotting force-extension traces for each specimen, averaging the energy absorbed across each configuration, and constructing a second-order 3D regression model to visualize the relationship. The regression model demonstrates a high level of agreement, with $R^2 = 0.94$ and $RMSE = 2166\,\mathrm{J}$. Ultimately, the coefficients of this model are evaluated using a coefficient F-Test with $p_d = 0.0033$, $p_t = 0.2319$, and $p_{td} = 0.0119$, leading to the rejection of the Null Hypothesis. While curvature in the unit cell density is significant, curvature in the isovalue alone is not, indicating that energy absorption is governed by coupled geometric effects rather than volume fraction itself.

Key words: gyroid, optimization, energy-absorption, instron-testing, hypothesis-testing, linear-regression

1 Introduction

The triply periodic minimal surface (TPMS), also known as the gyroid, is periodic in three independent directions with the symmetries of a crystallographic group. They are designed with lightweight and high strength that make them well suited for medical implants [1]. Their porous and biomimetic geometry closely mimic the mechanical behaviors of natural human bones. They can enhance biological fixation and reduce stress shielding and implant loosening with their interconnected pore network. These characteristics can lead to more stable orthopedic outcomes. In addition to medical implants, gyroids are used in additive manufacturing as architectural lattices that take advantage of 3D printing's design freedom. They can be fabricated from biodegradable polymers while maintaining structural integrity with modern 3D printing technology, such as fused deposition modeling (FDM). The ease of manufacturing makes them ideal for low-cost tissue engineering scaffolds [2]. Moreover, gyroids can serve as impact resistance structures. Utilizing their TPMS geometry in load bearing structures, loads can be efficiently distributed in a stable and energy-absorbing manner [3]. As one of the most advantageous properties a gyroid has, mechanical energy absorption is defined as the mechanical work performed during compression and is given by the integral of force over displacement:

$$E\,[\mathrm{J}] = \int \vec{F} \cdot d\vec{x} \tag{1}$$

The mechanical behavior of gyroids can be tuned by adjusting parameters, such as wall thickness and unit cell density. In order to obtain structures with good mechanical performance, the design optimization is essential for gyroid structures. For instance, some metamaterial structures based on gyroid-like unit cells achieve high mechanical strength obtained by large-scale diffusion generation models [4].

While combining gyroid generation based on Bézier curves with advanced optimization models like reinforcement learning gives a cutting edge method for topological optimization, this work focuses on the empirical characterization and prediction of optimization using a simple linear regression model. We propose an experimental approach to test the parameters that affect the mechanical behaviors of gyroids and then use a linear regression model to predict the optimal parameters experimented on. The gyroid structures will be precisely controlled by using the known[5] equation of a gyroid:

$$\sin(x)\cos(y) + \sin(y)\cos(z) + \sin(z)\cos(x) = T \tag{2}$$

The parameters we experimented on and varied are the isovalue T and the unit cell density d which is the number of identical unit cells per sample length. The goal of this study is to examine if there is a non-trivial relationship between these variables and energy absorption.

Since both parameters are likely to be proportional to volume fraction, a simple linear test would be insufficient. Thus, this study means to observe a quadratic or higher order behavior for energy absorption within the design space.

In order to collect the force-extension data, crush tests on an Instron are conducted while simultaneously measuring applied

load and displacement. If the following quadratic model is used to describe the energy absorbed (E) after a crush test with the following parameters (isovalue T and density d):

$$E(d,T) = \alpha + \beta_d d + \beta_t T + \gamma_d d^2 + \gamma_t T^2 + \delta t d \qquad (3)$$

Then, it is expected that the quadratic terms (γ_i) would be non-zero. This yields the following formal hypotheses, which can be tested by a Coefficient F-Test:

$$H_0 : (\gamma_t, \gamma_d) = (0,0)$$
$$H_1 : (\gamma_t, \gamma_d) \neq (0,0)$$

2 Methods

2.1 Model Generation

3D gyroid models were generated using a custom MATLAB script adapted from Rami Rouhana [6]. The implicit surface defined by Equation (2) was evaluated over a finite domain. For a unit cell density of d, the domain was defined as:

$$(x, y, z) \in [-d\pi,\, d\pi],$$

This corresponded to d repeated unit cells along each axis. The equation was then sampled on a uniform Cartesian grid with step size $\Delta = 0.05d$.

MATLAB's built-in `isosurface` and `isocaps` functions were then used to generate solid geometry, which was suitable for 3D printing. The scale was then reduced to 1"x1"x1", and an STL file was created and saved on the local hardware. An example of the configuration $T = 0.5$ and $d = [1, 2, 3]$ is shown in Figure 1

(Note: code for gyroid generation is viewable in Appendix A.)

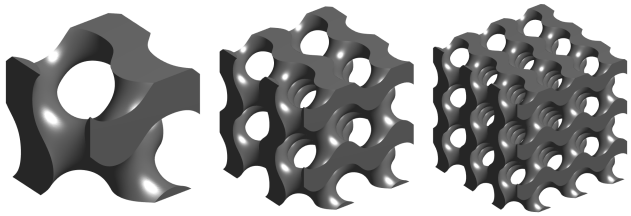

Figure 1: MATLAB generated gyroids of $T = 0.5$ and $d = [1, 2, 3]$.

The configurations tested in this study were all possible combinations of $T = \{0.25, 0.50, 0.75\}$ and $d = \{1, 2, 3\}$, forming a full-factorial 2-factor, 3-level experiment.

2.2 Sample Manufacturing

Fused deposition modeling (FDM) 3D printing was the main technique utilized during the fabrication process. All samples of interest were printed using a FlashForge Adventurer 5M FDM 3D printer. STL files corresponding to all nine design configurations were imported into OrcaSlicer slicing software to generate tool-paths at a layer height of $0.28\,\mathrm{mm}$. The print setup is shown in Figure 2

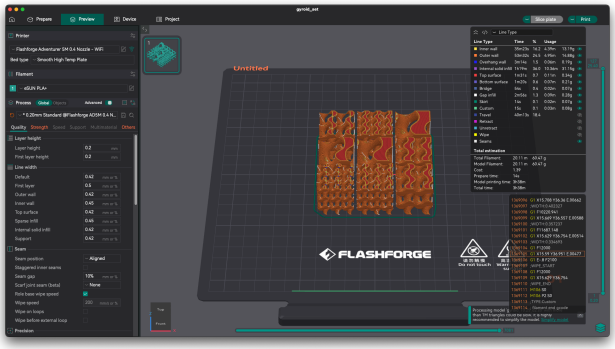

Figure 2: Screenshot of the OrcaSlicer software used to generate printer tool-paths.

All samples were printed using the same spool of white PLA filament on the same day in an air conditioned room where the temperature was set to $20\,^{\circ}\mathrm{C}$. In addition, print conditions were also controlled to be the same throughout the printing process, such as print speed and sample orientation. These intentional settings were meant to achieve the most consistency possible between printed samples to minimize random error from the manufacturing process.

This study used eSUN White PLA, though other brands would likely suffice. No post-processing was applied after printing, as it was determined that any artifacting due to lack of support would not contribute to loading paths during measurement. Each design configuration was fabricated with a replicate of three samples, producing a total of 27 printed samples. Figure 3 illustrates a successfully printed gyroid sample.

Figure 3: Representative 3D printed gyroid sample.

2.3 Instrument Calibration

Prior to crush testing, the Instron testing apparatus was calibrated to ensure accurate force and displacement measurements.

Load cell calibration was performed using a set of four known calibration weights of 50 lb each with a tolerance of ± 5 grains. The weights were applied incrementally to the load cell, and the measured loads were recorded to generate a calibration

curve relating the applied force to the instrument output.

Similarly, **extension (encoder) calibration** was conducted using a precision displacement gauge with a tolerance of ± 0.5 thou. A series of controlled travel steps were executed (each 100 thou), and the corresponding extension readings reported by the Instron were recorded and compared against the gauge measurements.

Both calibrations exhibited minimal deviation from one-to-one linearity, with negligible error observed across the tested ranges. As a result, the Instron system was deemed sufficiently accurate for subsequent compression testing without additional correction beyond linear calibration factors.

2.4 Instron Crush Testing

As mentioned in the Introduction, the energy absorbed through mechanical work can be interpreted as the integral of force over the distance traveled as shown in Figure 4.

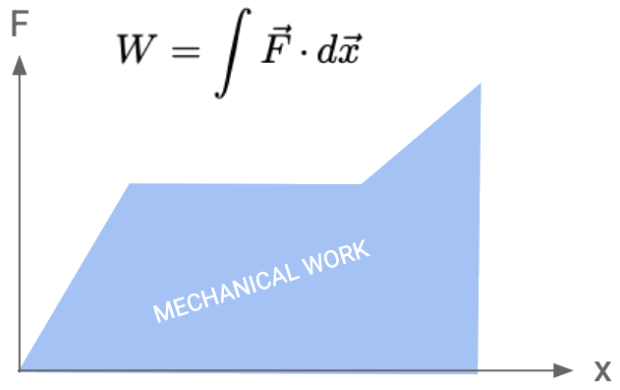

Figure 4: Energy absorption from the Instron represented as the blue area under the load–displacement curve.

The Instron present in Hesse Hall offered a great avenue for carrying this out. Figure 5 shows a 2D schematic of the Instron testing apparatus:

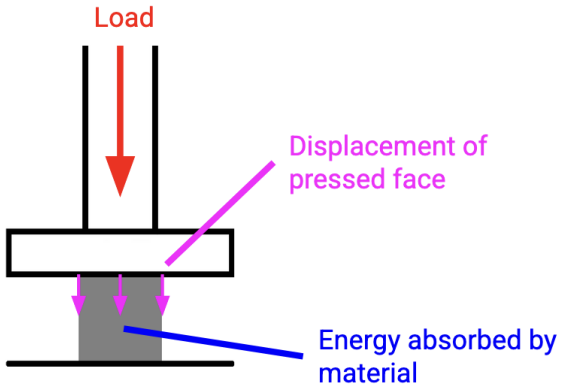

Figure 5: 2D Schematic of Instron Testing Procedure

A total of 27 samples with three replicates per configuration were tested under identical loading conditions using a custom compression method. For each test, the following procedure was observed:

1. Move top platter to a height of 1.00" (25.4 mm)
2. (If present) remove old sample
3. Place fresh sample centered on platter, with layer lines parallel to the floor.
4. Move top platter downward at a rate of 10 mm/min, until an extension of at least 15mm is achieved.
5. Record data, repeat steps 1-5 if uncrushed samples remain.

Figure 6 shows the 27 crushed samples. Each sample was deformed in the longitudinal axis by at least $15mm$. It was observed that with a low isovalue, the samples tend to fracture internally while samples with a higher isovalue deformed more as a whole. We attributed this interesting finding to the fact that samples with a higher isovalue had better tensegrity that can help them hold their internal structure and therefore prevent internal fractures.

Figure 6: The 27 crushed gyroids after testing.

The orders of testing were summarized in Table 1 below:

Sample Number	Isovalue t	Cell Density
1–3	0.25	1 unit
4–6	0.25	2 units
7–9	0.25	3 units
10–12	0.5	1 unit
13–15	0.5	2 units
16–18	0.5	3 units
19–21	0.75	1 unit
22–24	0.75	2 units
25–27	0.75	3 units

Table 1: Our 3x3 Experimental design with Run Numbers and parameter combinations.

2.5 Data Processing and Hypothesis Testing

Raw load–displacement data from Instron compression tests were exported to CSV files and processed using a custom MATLAB script. Each file contained time-series measurements of top-surface displacement and applied force for a single sample.

Mechanical energy absorption was then computed for each sample by numerically integrating force with respect to

displacement using the trapezoidal rule,

$$E = \int F\,dx \tag{4}$$

as implemented by MATLAB's `trapz` function.

For each combination of isovalue and unit cell density, three replicate measurements were obtained. Energy absorption values were stored in an array indexed as $(d, t, \text{replicate})$, and the mean energy absorption was computed across replicates for visualization and regression analysis.

To observe trends within the design space, second-order polynomial regressions were fitted independently in the d- and t-planes, as well as jointly across both parameters. A quadratic surface model of the form

$$E(d,t) = \alpha + \beta_d d + \beta_t t + \gamma_d d^2 + \gamma_t t^2 + \delta dt \tag{5}$$

was fitted using the least squares method via MATLAB's built-in `fitlm` function.

Statistical significance of the quadratic coefficients was found using the coefficient F-test on the quadratic terms. Individual hypotheses $\gamma_d = 0$ and $\gamma_t = 0$, as well as the joint hypothesis $(\gamma_d, \gamma_t) = (0, 0)$, were tested using MATLAB's built-in `coefTest` function.

This was determined to be the appropriate hypothesis test, as it compared the variance explained by individual linearly-independent components of the model with all other terms in the model.[7]

3 Results

It is noted that both sensors on the Instron present a nearly one-to-one linear calibration curves.

However, uncertainty grows with each mass placed on the load cell since the uncertainty of each calibration mass is independent. However it is constant for the extension.

Figure 7 displays the calibration results for both sensors on the Instron apparatus:

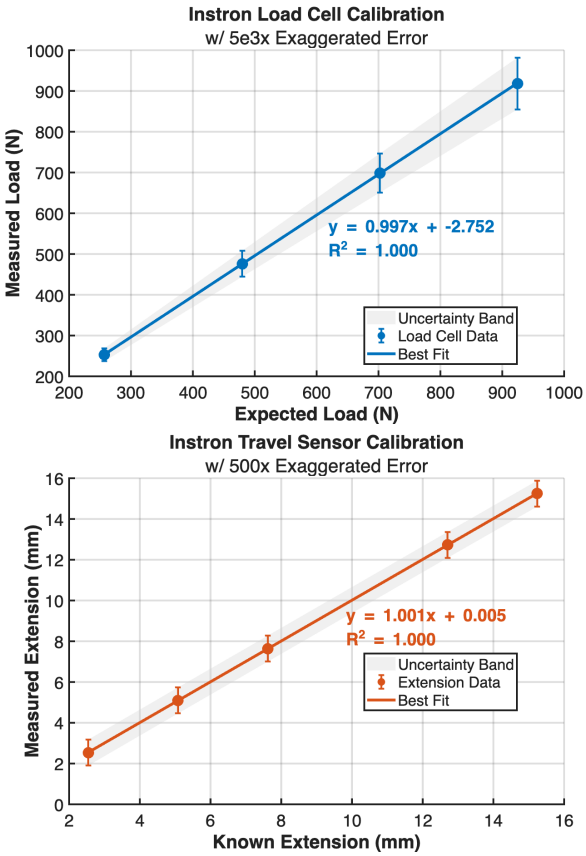

Figure 7: Instron calibration results. Note: error bars are grossly exaggerated to draw attention to the shape of the uncertainty

Plotting the raw data obtained from the Instron, Figure 8 shows the traces of Force-Displacement for the 27 samples:

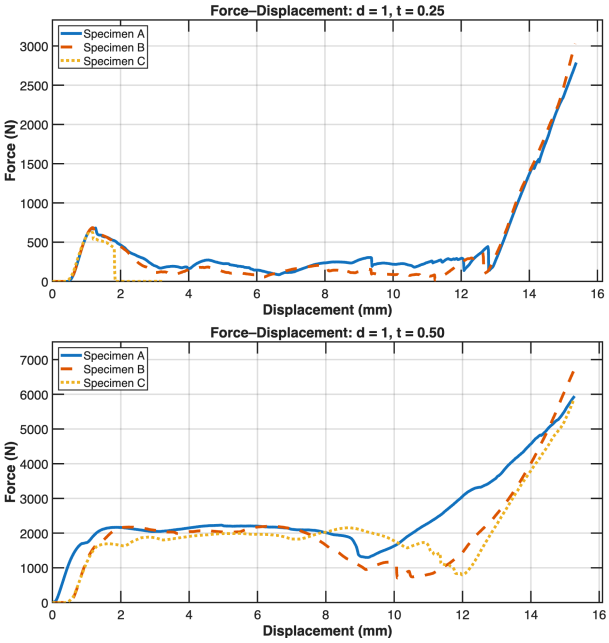

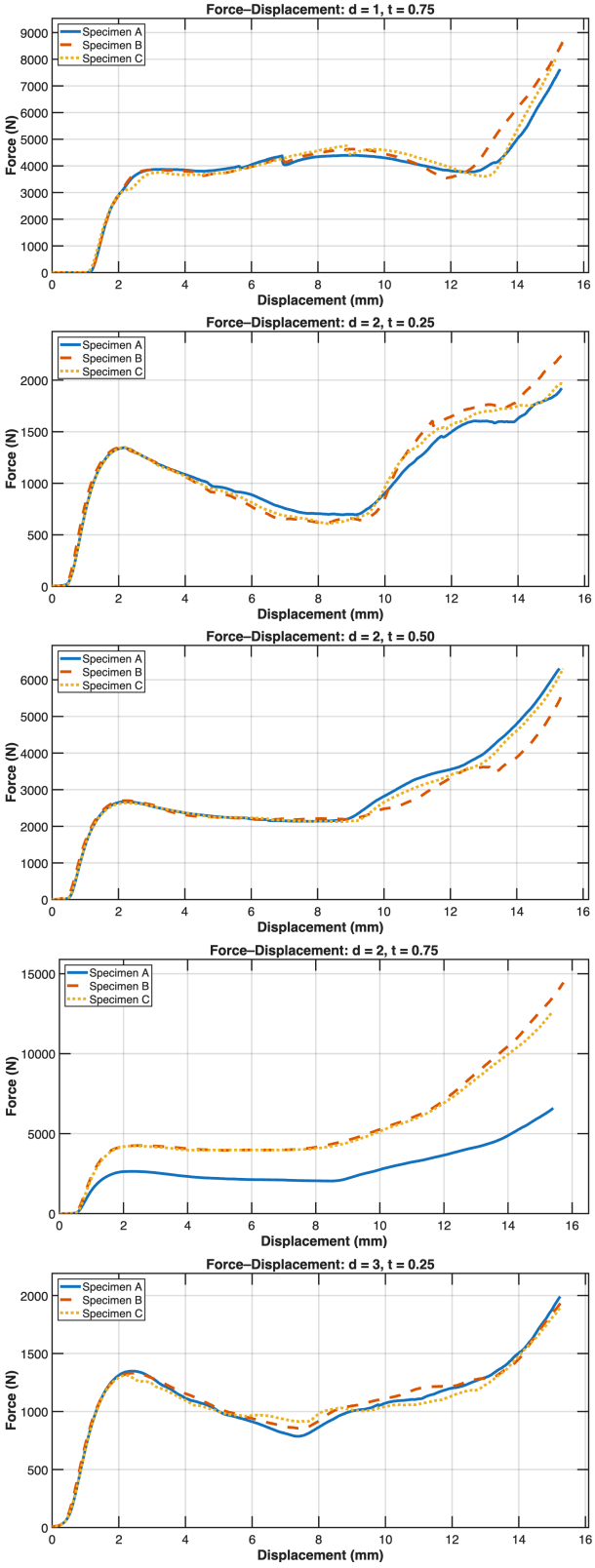

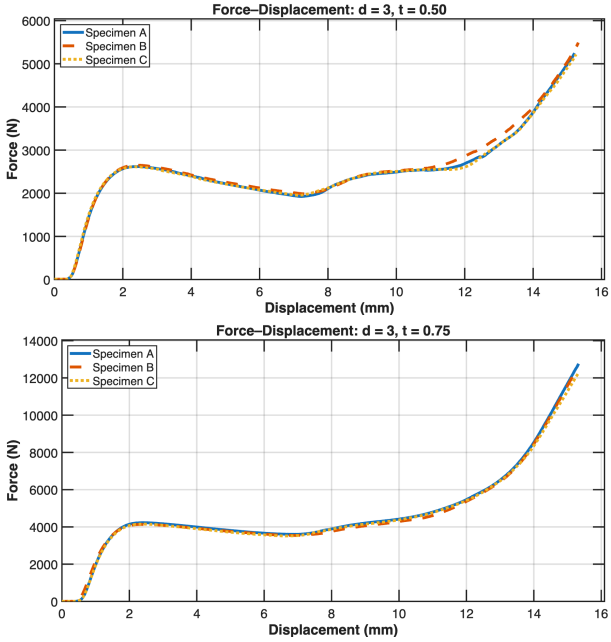

Figure 8: Force–extension traces for all 27 gyroids

These traces were first integrated to compute the energy absorbed for each sample, and the average value was then taken to represent the energy absorption for each configuration. Finally, the average energy absorption results were used to create a quadratic model as shown in 9.

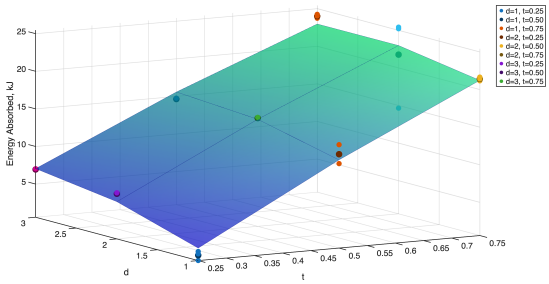

Figure 9: 3D Quadratic Regression of Gyroid Energy Absorption vs. Thickness t and Cell Density d.

The surface can be separated and viewed from the t- and d- planes independently. Regression models were generated to reveal a more comprehensive relationship between these two parameters and the energy absorption of gyroids as shown in Figure 10.

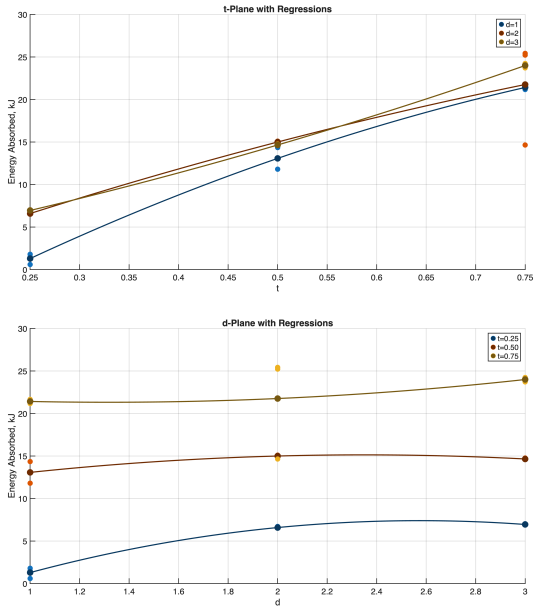

Figure 10: 2D Cross-Sections of the 3D Isosurface of $E(t, d)$.

As the last step, a hypothesis test is performed using MATLAB's `coeffTest` with a significance of $\alpha = 0.05$. The results are summarized in Table 2 below:

Test	H_0	p-value	Reject H_0?
d-curvature	$\gamma_d = 0$	0.0033	Yes
t-curvature	$\gamma_t = 0$	0.2319	No
Joint curvature	$\gamma_d = \gamma_t = 0$	0.0119	Yes

Table 2: Coefficient F-tests for quadratic terms in the model.

4 Discussion

The results of this study confirm the existence of a "sweet spot" in regards to gyroid energy absorption within our design space (isovalue and cell density), rather than scaling linearly with volume fraction alone.

The fitted quadratic surface achieved strong agreement with the experimental data ($R^2 = 0.94$, $RMSE = 2166\,\mathrm{J}$). Visual inspection implied the quadratic nature of this behavior, with confirmation from statistical tests proving the formal hypothesis.

However, while the second-order model implied that quadratic curvature was significant in the density alone (γ_d) and the isovalue-density joint interaction ($\gamma_d\gamma_t$ were statistically significant, the isovalue (γ_t) alone proved to be a linear (i.e. trivial) relationship only. This non-triviality agrees with prior literature [3], despite differences in test set-up (e.g. sheet vs. solid gyroids, impact vs crush testing).

Intuitively, the results make sense. Increasing the unit cell density increases the number of load paths, but overly increasing it makes the walls too thin. Meanwhile, increasing the isovalue on a solid gyroid is simply akin to increasing the volume fraction.

This result is consistent with prior observations in literature. A study by Ramos et. al. found a similar non-triviality, despite using a slightly different setup with sheet gyroids undergoing impact rather than solid gyroids undergoing crushing.

4.1 Limitations and Sources of Error

Despite the statistical significance of the model's curvature, this study does not claim to have identified a global optimum within the design space. The limited number of configurations in combination with the modest number of replicates due to limited time on the Instron limit the resolution of the regressed iso-surface.

Additionally, the limitations of FDM 3D printing should not be left unacknowledged. Due to time constraints, the specimens needed to be printed at a scale of 1"x1"x1", despite an original intended scale of 2"x2"x2". This caused the layer-lines to be locally larger and impacted the behavior of the structures.

If the experiment were to be improved, it would be better to use more precise manufacturing methods, such as SLA 3D printing, which would allow a significantly higher layer-line resolution, resulting in lower influence from the layer lines.

These aforementioned limitations are likely the cause of anomalies, such as the very-quickly-failing Specimen C in the $(d = 1, t = 0.25)$ trace. It was noted that samples with lower isovalues/densities tended to fail due to separation of the layers, while samples with higher isovalues/densities failed due to a more natural "squishing" failure mode.

However, this is the reason the study's hypothesis is so specifically chosen. To mitigate the limitations of the manufacturing methods, the study only aimed to identify **if a trend exists.**

4.2 Future Research

Due to time constraints, the study had a very limited amount of specimens/levels of redundancy available to test. If more time were allotted, the group would have likely created more specimens at different scales, using normalized energy units to truly probe if the non-linear relationship is based on geometry alone.

Further analysis could result in scripting/software tools that could suggest which designs to test next, in search of a true optimum (as opposed to continuing along a fixed factorial design).

Increasing experimental redundancy would further strengthen statistical confidence in the results.

Finally, incorporating numerical simulation methods, such as finite element modeling, along with non-parametric alterations on the geometry could present an interesting avenue of study. This would allow for further insight into the failure modes and an expanded design space in search of a true optimum.

5 Conclusion

The study examines how gyroid geometry influences mechanical energy absorption by varying the isovalue and the unit cell density under controlled crush testing.

Experimental data and testing of the formal hypothesis did indeed demonstrate that this relationship exists and is non-trivial / non-linear. Instead, statistical coefficient F-testing confirms a significant non-linear interaction between the isovalue and the unit cell density, indicating that gyroid performance is governed by coupled geometric mechanisms. The quadratic regression model captured these trends well, and the associated hypothesis tests verified that the observed curvature is not the result of experimental noise.

From a design perspective, these findings suggest that gyroids can be optimized through geometry rather than by increasing density or thickness alone. Even within a limited design space and with modest replication, clear trends emerge that highlight the importance of parameter interaction in energy-absorbing structures.

6 Acknowledgments

The authors would like to thank the **ME103 Course Staff**, and especially **Panithan Lertsuntivit**, for his excellent guidance in narrowing the project scope and refining for suitability for ME103.

We would also like to thank **Daniel Paragas** from Hesse Hall for his assistance/tutorial in setting up the Instron machine.

Finally, thanks to **The MathWorks Team** for excellent documentation which assisted in deciding relevant hypothesis testing and **Rami Rouhana** on YouTube for helpful tutorial on creating gyroid STL files in MATLAB.

7 Works Cited

References

[1] B. Eltlhawy, N. Fouda, and I. Eldesouky, "Numerical evaluation of a porous tibial-knee implant using gyroid structure," *Journal of Biomedical Physics and Engineering*, vol. 12, no. 1, p. 75, 2022.

[2] L. Germain, C. A. Fuentes, A. W. van Vuure, *et al.*, "3d-printed biodegradable gyroid scaffolds for tissue engineering applications," *Materials & Design*, vol. 151, pp. 113–122, 2018.

[3] H. Ramos, R. Santiago, S. Soe, *et al.*, "Response of gyroid lattice structures to impact loads," *International Journal of Impact Engineering*, vol. 164, p. 104202, 2022.

[4] Y. Jadhav, J. Berthel, C. Hu, *et al.*, "Generative lattice units with 3d diffusion for inverse design: Glu3d," *Advanced Functional Materials*, p. 2404165, 2024.

[5] L. Bu, "Modeling the gyroid in geogebra," *North American Geogebra Journal*, vol. 12, 2024.

[6] R. Rouhana, "Generate gyroid structures using matlab (meshlab +freecad conversion)." `https://www.youtube.com/watch?v=uvCfVsFAcSw`, 2022.

[7] MathWorks, "coeftest: Linear hypothesis test on linear regression model coefficients." `https://www.mathworks.com/help/stats/linearmodel.coeftest.html`. Accessed: 15 Dec. 2025.

Appendix A: GYROID STL GENERATION SCRIPT

Listing 1: MATLAB script used to generate solid gyroid geometries.

```
% Authors: Eyan Documet
% Reference: Rami Rouhana
% https://www.youtube.com/watch?v=uvCfVsFAcSw

% -- Example usage: --
clear all; close all; clc

T = 0.75;
density = 2;

[V, F] = gen_gyroid(T, density);
plot_gyroid(V, F);


% -- Functions: Generation, Saving, and Plotting -- %
function [V,F] = gen_gyroid(T, density)
    % Setup
    step = 0.05*density;
    L = -density*pi:step:density*pi;
    [X, Y, Z] = meshgrid(L);

    % From Wikipedia, well known
    Gyroid = cos(X).*sin(Y) + cos(Y).*sin(Z) + cos(Z).*sin(X) + T;

    % Generating surface mesh
    [F1, V1] = isosurface(X, Y, Z, Gyroid, 0);
    [F2, V2] = isocaps(X, Y, Z, Gyroid, 0, 'below');

    F = [F1; F2 + size(V1, 1)];
    V = [V1; V2];

    % Scale to 25.4 mm cube
    sizeXYZ = max(V) - min(V);           % current dimensions
    scaleFactor = 25.4 ./ max(sizeXYZ);  % uniform scale
    V = V * scaleFactor;
end

function plot_gyroid(V,F,filename)
    if nargin < 3
        filename = 'gyroid_plot.png';
    end

    figure;
    patch('Vertices',V,'Faces',F,'FaceColor','#808080','EdgeColor','none');
    axis off; axis equal; view(3); camlight; lighting gouraud;
    set(gca,'Visible','off');
    set(gcf,'Color','white');
    exportgraphics(gcf, filename, 'BackgroundColor','white');
end

function save_gyroid(V,F,filename)
    if nargin < 3
        filename = 'gyroid.stl';
    end

    TR = triangulation(F,V);
    stlwrite(TR, filename);
end
```